Adaptive Central-Upwind Schemes for Hyperbolic Systems of Conservation Laws

Lucian A. Constantin and Alexander Kurganov

Abstract. Central-upwind schemes, recently introduced in [7, 8], are simple, universal, and efficient Godunov-type projection-evolution methods for hyperbolic systems of conservation laws. Their efficiency, however, is typically reduced at the projection step, which requires nonlinear limiters to prevent oscillations. Such limiters, especially those that are higher than second order accurate, are computationally expensive. They may also cause excessive smearing of (liner) contact waves.

We present a new adaptive version of the central-upwind schemes, in which second-order limiters are applied near shock waves only, while in the rest of the computational domain, an unlimited fifth-order reconstruction is employed. Our adaption strategy is based on the modified version of the weak local residual from [5], which is used to automatically distinguish between shock and contact discontinuities.

1. Introduction

We consider one-dimensional hyperbolic systems of conservation laws:

$$u_t + f(u)_x = 0. \tag{1}$$

It is well-known that solutions of such systems may develop discontinuities even when the initial data, $u_0(x) := u(x,0)$ are smooth. This makes developing high-resolution non-oscillatory numerical methods for (1) a very challenging task.

In this paper, we focus on Godunov-type projection-evolution methods, in which a piecewise polynomial interpolant is first reconstructed from the cell averages, computed at some time level, and is then evolved to the next time level according to the integral form of the conservation law.

Classical Godunov-type schemes are upwind, since their evolution step requires solving (generalized) Riemann problems (see, e.g., [1, 10, 17]), and this may be

rather complicated. Godunov-type central schemes offer a much simpler and universal alternative approach, where, due to averaging over the Riemann fans, no Riemann problem solver or characteristic decomposition is involved (see, e.g., [7, 8, 11, 15]).

High-order Godunov-type schemes — both upwind and central ones — achieve high resolution with the help of high-order piecewise polynomial reconstructions. However, such reconstructions may generate oscillations unless nonlinear limiters are used in the computation of polynomial pieces. There is a library of reliable second-order piecewise linear reconstructions (see, e.g., [9, 12, 15, 16]). Higher-order reconstructions has also been intensively studied (see, e.g., [4, 11, 13, 14]), but they are much more complicated and computationally expensive.

We would like to emphasize that while the nonlinear limiters help to prevent oscillations near discontinuities, the use of limiters in smooth areas is redundant — it dramatically reduces the efficiency of the method and may also cause a loss of resolution. This leads to the idea of scheme adaption, implemented in the context of the Godunov-type central schemes in [6]: using a smoothness indicator detect "rough" parts of the computed solution and apply limiters only there.

The main goal of this paper is to develop an improved adaptive scheme, in which (nonlinear) shock and (linear) contact waves will be treated differently: limiters are applied only near the shocks (in fact, the use of computationally inexpensive piecewise linear reconstruction is typically sufficient to accurately capture shock waves), while in the rest of the computational domain a higher-order "unlimited" scheme is used. The latter may result in some oscillations near contact waves and rarefaction corners, but their amplitude is rather small and a non-oscillatory solution can be recovered, for example, by a nonlinear filter from [2], applied as a post-processing.

The key point of our approach is how to automatically distinguish between shock and contact discontinuities. It is clear that this cannot be done by a smoothness indicator based on a pure data analysis. To achieve our goal, we have implemented a modified version of a smoothness indicator (SI) recently proposed in [5]. This SI is based on a weak local residual, which, in fact, indicates the quality of the computed solution — not only its local smoothness. As it was demonstrated in [5] and also supported by our numerical results, the size of this SI at shock and contact waves is typically so different that one can easily detect immediate shock vicinities, where the limiters are to be applied.

We have chosen the semi-discrete central-upwind scheme from [7] as an underlying method for our adaption algorithm. However, we would like to point out that our adaptive method is not tied to a specific choice of an underlying scheme and can be implemented with one's favorite methods.

2. Semi-Discrete Central-Upwind Schemes — an Overview

We consider a uniform spatial grid $x_\alpha := \alpha\Delta x$ and assume that at a certain time level t we have computed an approximate solution, realized in terms of its cell averages: $\bar{u}_j(t) \approx \bar{u}(x_j,t) = \frac{1}{\Delta x}\int_{x_{j-\frac12}}^{x_{j+\frac12}} u(\xi,t)\,d\xi$. Using these data, we first reconstruct a conservative non-oscillatory piecewise polynomial interpolant: $\widetilde{u}(x,t) := \sum_j p_j(x,t)\chi_j(x)$, where χ_j is the characteristic function of the interval $[x_{j-\frac12}, x_{j+\frac12}]$, and $p_j(x,t)$ is the corresponding polynomial piece on this interval. A (formal) spatial order of accuracy of the resulting central-upwind scheme is, in fact, determined by the order of the interpolant. For example, a second-order scheme requires a second-order piecewise linear reconstruction, whose slopes are to be computed using a nonlinear limiter to ensure a non-oscillatory nature of the reconstruction. In this paper, we use the minmod limiter (consult, e.g., [9, 15, 16]).

The piecewise polynomial interpolant $\widetilde{u}(x,t)$ is then evolved in time according to the central-upwind semi-discrete scheme:

$$\frac{d}{dt}\bar{u}_j(t) = -\frac{H_{j+\frac12}(t) - H_{j-\frac12}(t)}{\Delta x}, \tag{2}$$

where the numerical fluxes are

$$H_{j+\frac12}(t) := \frac{a^+_{j+\frac12} f(u^-_{j+\frac12}) - a^-_{j+\frac12} f(u^+_{j+\frac12})}{a^+_{j+\frac12} - a^-_{j+\frac12}} + \frac{a^+_{j+\frac12} a^-_{j+\frac12}}{a^+_{j+\frac12} - a^-_{j+\frac12}}\left[u^+_{j+\frac12} - u^-_{j+\frac12}\right]. \tag{3}$$

Here, $u^+_{j+\frac12} := p_{j+1}(x_{j+\frac12},t)$ and $u^-_{j+\frac12} := p_j(x_{j+\frac12},t)$ are the corresponding right and left values of the interpolant at the cell interface $x = x_{j+\frac12}$, and $a^+_{j+\frac12}$ ($a^-_{j+\frac12}$) are the right-sided (left-sided) local speeds of propagation, which are related to the largest and the smallest eigenvalues of the Jacobian $\frac{\partial f}{\partial u}$ at $x = x_{j+\frac12}$, see [7].

Remark. The semi-discretization (2)–(3) results in a system of ODEs, which should be numerically integrated by an appropriate ODE solver. In our numerical experiments, we have used the fourth-order SSP Runge-Kutta method from [3].

3. Weak Smoothness Indicator

In this section, we describe a smoothness indicator (SI) used in our adaptive algorithm. This SI is a modified version of the SI from [5, 6].

Since solutions of hyperbolic conservation laws are typically discontinuous, they are understood as weak solutions in the sense of distributions. By definition, a weak solution $u(x,t)$ of (1) satisfies the following integral identity:

$$E(u,\Phi) = -\int\limits_{t=0}^{\infty}\int\limits_{X}\{u(x,t)\Phi_t(x,t) + f(u(x,t))\Phi_x(x,t)\}\,dxdt + \int\limits_{X} u(x,0)\Phi(x,0)\,dx = 0 \tag{4}$$

for all test functions $\Phi(x,t) \in C_0^\infty(X \times [0,\infty])$. The key idea in [5] was to develop an indicator that checks by how much the computed solution, denoted by u^Δ, fails to satisfy (4).

However, it is obvious that $E(u^\Delta, \Phi)$ can not be computed for every Φ in practice. Thus, the next step in the construction of the SI is replacing $\Phi(x,t)$ with a concrete set of localized test-functions $\Phi_j^n(x,t)$. In [5], a particular choice of $\Phi_j^n(x,t)$ was the local quadratic B-splines, which satisfy appropriate approximation properties. The resulting expressions $E(u^\Delta, \Phi_j^n)$ are, in fact, weak local residuals, which, as it was demonstrated in [5, 6], can be used as a SI.

Here, we construct a simpler and less computationally expensive modification of the SI, obtained via the localized test-functions $\Phi_{j+\frac12}^{n-\frac12}(x,t) = B_{j+\frac12}(x)B^{n-\frac12}(t)$, where $B_{j+\frac12}(x)$ and $B^{n-\frac12}(t)$ are the quadratic B-splines, centered at $x = x_{j+\frac12}$ and $t = t^{n-\frac12}$, with supports of size $2\Delta x$ and $2\Delta t$. The weak local residual $E_{j+\frac12}^{n-\frac12} := E(u^\Delta, \Phi_{j+\frac12}^{n-\frac12})$ is then calculated straightforwardly and it is equal to:

(5)
$$E_{j+\frac12}^{n-\frac12} = \frac{1}{2}\left\{\Delta x\left[u_j^n - u_j^{n-1} + u_{j+1}^n - u_{j+1}^{n-1}\right] + \Delta t\left[f(u_{j+1}^{n-1}) - f(u_j^{n-1}) + f(u_{j+1}^n) - f(u_j^n)\right]\right\},$$

where u_j^n are the point values of the computed solution. Note that this version of the weak local residual uses a 2×2 stencil, compared with the 3×3 stencil used in the original SI in [5] (it is thus less computationally expensive).

The error analysis and the numerical experiments in [5] suggest that for a convergent numerical method of (a formal) order r, one should expect to have

$$|E_{j+\frac12}^{n-\frac12}(x)| = \begin{cases} O(\Delta), & \text{near shocks,} \\ O(\Delta^\alpha), & \text{near contact discontinuities, } 1<\alpha\le 2, \\ O(\Delta^{\min(4,r+2)}), & \text{in the smooth regions.} \end{cases} \tag{6}$$

Here, $\Delta \equiv \max(\Delta x, \Delta t)$, and α depends on the quality of the contact wave resolution. The results of our numerical experiments with the modified SI (5) are consistent with the estimate (6). In particular, we have observed that the values of the SI near contact waves are typically much smaller than its values near shocks. This feature of the SI is one of the key points of our adaptive algorithm, because at every time level we first check the location of shocks, and then the "limited" central-upwind scheme is applied only in the vicinities of shocks, while the remaining part of the solution (including the contact regions) is treated by a higher-order "unlimited" scheme.

4. Adaptive Central-Upwind Schemes

In this section, we present a new scheme adaption technique, whose key steps are:

1. Detect shock regions and apply a "limited" second-order scheme there.
2. Elsewhere, apply a (linear) "unlimited" high-order scheme.
3. If necessary, post-process the final results by a filter to remove oscillations.

STEP 1: SHOCK DETECTION ALGORITHM. Assume that we compute a piecewise smooth solution with (at most) a finite number of shocks and contact discontinuities. Then, according to (6), we expect to have:

$$\begin{aligned}\frac{1}{\Delta x}\|E^{n-\frac12}\|_1 &= \sum_{x_{j+\frac12}\in\Omega_1}|E^{n-\frac12}_{j+\frac12}|+\sum_{x_{j+\frac12}\in\Omega_2}|E^{n-\frac12}_{j+\frac12}|+\sum_{x_{j+\frac12}\notin(\Omega_1\cup\Omega_2)}|E^{n-\frac12}_{j+\frac12}|\\ &\simeq C_1\Delta+C_2\Delta^{\alpha}+\mathrm{O}(\Delta^{\min(3,r+1)}),\quad \alpha\in(1,2],\end{aligned}\tag{7}$$

where Ω_1 (Ω_2) is a union of the shock (contact) regions, the constants C_1 and C_2 are proportional to the number of shock and contact discontinuities, respectively, and r is a formal order of the method.

The estimate (7) implies that as $\Delta\sim 0$, only those values of $|E^{n-\frac12}_{j+\frac12}|$ that are near shocks will be larger than $\|E^{n-\frac12}\|_1$, and this will allow one to distinguish between the shock regions and the remaining parts of the solution. However, in practice we cannot take Δ to be too small and therefore we have to adjust our adaption strategy by introducing an adaption constant K and then making the following conclusion:

$$\begin{array}{ll}\text{if } |E^{n-\frac12}_{j+\frac12}|\ge K\|E^{n-\frac12}\|_1, & \text{then } (x_{j+\frac12},t^n) \text{ is in the shock region,}\\ \text{otherwise,} & (x_{j+\frac12},t^n) \text{ is outside of the shock region.}\end{array}\tag{8}$$

STEP 2: "UNLIMITED" HIGH-ORDER CENTRAL SCHEME. Away from the shock regions, identified in Step 1, we use of the central-upwind scheme (2)–(3) with an unlimited fifth-order reconstruction, realized by the fourth-degree polynomial pieces p_j, whose coefficients are obtained from the following conservation requirements:

$$\bar u_{j\pm l}(t)=\frac{1}{\Delta x}\int\limits_{x_{j\pm l-\frac12}}^{x_{j\pm l+\frac12}}p_j(x,t)\,dx,\quad l=0,1,2.$$

In order to illustrate a high potential of the "unlimited" scheme, we demonstrate its performance on an example of a single slow moving contact discontinuity. We consider the Euler equations of gas dynamics:

$$\frac{\partial}{\partial t}\begin{pmatrix}\rho\\ m\\ E\end{pmatrix}+\frac{\partial}{\partial x}\begin{pmatrix}m\\ \rho u^2+p\\ u(E+p)\end{pmatrix}=0,\qquad p=(\gamma-1)(E-\frac{\rho u^2}{2}),\tag{9}$$

where $\rho, u, m=\rho u, p$, and E are the density, velocity, momentum, pressure, and total energy; subject to the following initial data:

$$(\rho,u,p)(x,0)=\begin{cases}(1.4,0.1,1), & \text{if } x<0.5,\\ (1.0,0.1,1), & \text{if } x>0.5.\end{cases}\tag{10}$$

In Figure 1(left), we plot the numerical solutions at time $t=2$, computed by the "limited" second-order central-upwind scheme from [7] and its fifth-order "unlimited" sibling (in both cases, $\Delta x=0.005$). One can clearly see that the "unlimited"

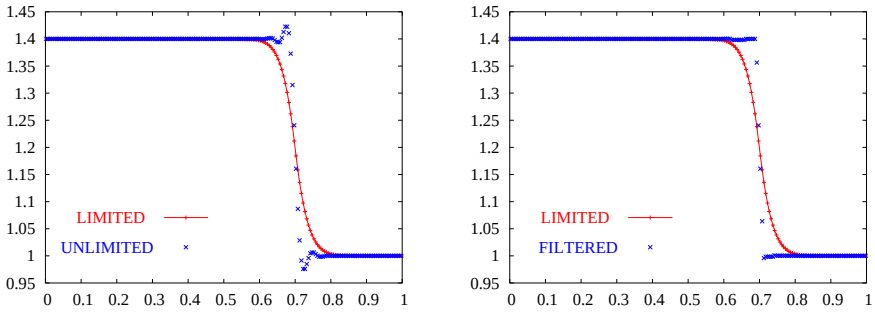

FIGURE 1. Moving contact discontinuity by the second-order "limited" and the original (left) and filtered (right) fifth-order "unlimited" central-upwind schemes.

scheme provides an improved resolution of the contact discontinuity, while producing some oscillations.

STEP 3: NONLINEAR FILTERS. The oscillations caused by the application of "unlimited" scheme near contact discontinuities and rarefaction corners can be removed, for example, with the help of the nonlinear filter proposed in [2], applied as a post-processing.

Let consider the previous example of a slow moving contact wave. If the "unlimited" results, shown in Figure 1(left), are post-processed by the filter, the oscillations are almost completely removed, while the quality of the resolution of the contact wave remains extremely high, see Figure 1(right).

Remark. It may happen that $E^{n-\frac{1}{2}}_{j+\frac{1}{2}}$ changes sign inside the shock vicinity, such that for some j_0 there, $|E^{n-\frac{1}{2}}_{j_0+\frac{1}{2}}| \sim 0$. In order to guarantee that the shock vicinity is robustly detected, we first apply a standard smoothing procedure to the computed values of $|E^{n-\frac{1}{2}}_{j+\frac{1}{2}}|$ and then extend the "shock areas", detected based on the smoothed values of $|E^{n-\frac{1}{2}}_{j+\frac{1}{2}}|$, by few more cells.

5. Numerical Experiments

In this section, we present two numerical experiments, illustrating the performance of the proposed adaptive central-upwind scheme. In both examples, $\Delta x = 0.005$ and the adaption constant in (8) is $K = 10$.

Example 1 — Toro's Version of the Sod Problem. We numerically solve the Euler equations of gas dynamics (9) subject to the following initial data [17]:

$$(\rho, u, p)(x, 0) = \begin{cases} (1.000, 0.75, 1.0), & \text{if } x < 0.3, \\ (0.125, 0.00, 0.1), & \text{if } x > 0.3. \end{cases} \tag{11}$$

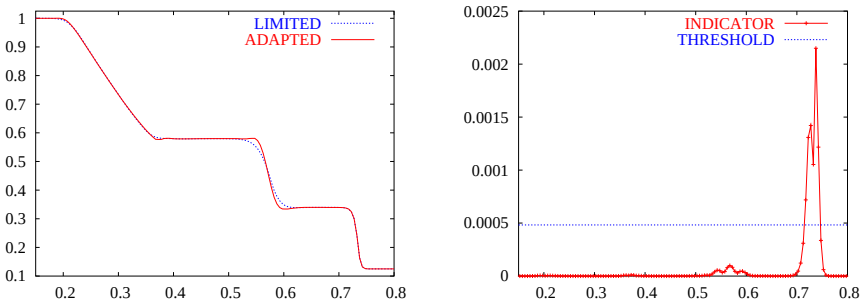

FIGURE 2. Solutions of (9),(11) by the second-order and adaptive central-upwind schemes (left) and the SI values (right).

The numerical solutions at time $t = 0.2$, computed by the original second-order central-upwind scheme and its adaptive modification are shown in Figure 2(left). One can observe an improved resolution of the contact discontinuity, achieved by our adaptive scheme. In Figure 2(right), we show the values of $\frac{1}{\Delta x}|E_{j+\frac{1}{2}}|$ and the adaption threshold $K\|E\|_1$, computed at the final time. This plot illustrates the ability of our SI to distinguish between the shock and contact discontinuities.

Example 2 — Three Discontinuities Traveling to the Right. In this example, also taken from [17], we numerically solve the system (9) subject to the different initial data:

$$(\rho, u, p)(x, 0) = \begin{cases} (5.99924, 19.5975, 460.894), & \text{if } x < 0.4, \\ (5.99242, -6.19633, 46.0950), & \text{if } x > 0.4. \end{cases} \tag{12}$$

The final time is 0.035.

As in Example 1, the application of our scheme adaption strategy leads to an improved resolution of the contact wave, see Figure 3(left), since no limiters are applied in its vicinity, where the value of the SI is much smaller than the ones at the shocks, see Figure 3(right).

Acknowledgment: The work of L. Constantin and A. Kurganov was supported in part by the NSF Grant # DMS-0310585.

References

[1] M. Ben-Artzi and J. Falcovitz, *Generalized Riemann problems in computational fluid dynamics*, Cambridge University Press, 2003.

[2] B. Engquist, P. Lotstedt and B. Sjogreen, *Nonlinear filters for efficient shock computation*, Math. Comp., 52 (1989), pp. 509–537.

[3] S. Gottlieb, C.-W. Shu and E. Tadmor, *High order time discretization methods with the strong stability property*, SIAM Rev., 43 (2001), pp. 89–112.

[4] A. Harten, S. Osher, B. Engquist and S.R. Chakravarthy, *Some results on uniformly high order accurate essentially non-oscillatory schemes*, Appl. Numer. Math., 2 (1986), pp. 347–377.

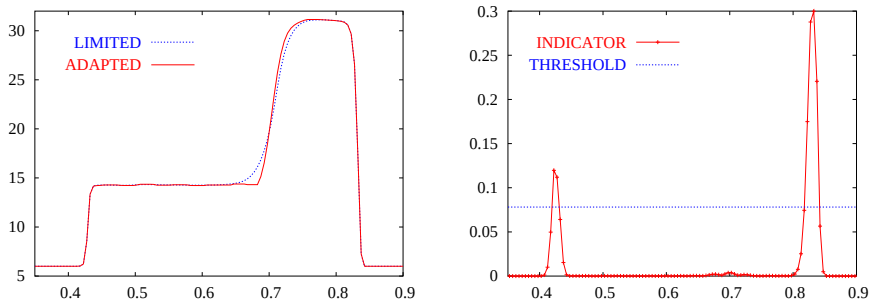

FIGURE 3. Solutions of (9),(12) by the second-order and adaptive central-upwind schemes (left) and the SI values (right).

[5] S. KARNI AND A. KURGANOV, *Local error analysis for approximate solutions of hyperbolic conservation laws*, Adv. Comput. Math., 22 (2005), pp. 79–99.
[6] S. KARNI, A. KURGANOV AND G. PETROVA, *A smoothness indicator for adaptive algorithms for hyperbolic systems*, J. Comput. Phys., 178 (2002), pp. 323–341.
[7] A. KURGANOV, S. NOELLE AND G. PETROVA, *Semi-discrete central-upwind scheme for hyperbolic conservation laws and Hamilton-Jacobi equations*, SIAM J. Sci. Comput., 23 (2001), pp. 707–740.
[8] A. KURGANOV AND E. TADMOR, *New high-resolution central schemes for nonlinear conservation laws and convection-diffusion equations*, J. Comput. Phys., 160 (2000), pp. 241–282.
[9] B. VAN LEER, *Towards the ultimate conservative difference scheme, V. A second order sequel to Godunov's method*, J. Comput. Phys., 32 (1979), pp. 101–136.
[10] R. LEVEQUE, *Finite volume methods for hyperbolic problems*, Cambridge Texts in Applied Mathematics, Cambridge University Press, 2002.
[11] D. LEVY, G. PUPPO AND G. RUSSO, *Central WENO schemes for hyperbolic systems of conservation laws*, M2AN Math. Model. Numer. Anal., 33 (1999), pp. 547–571.
[12] K.-A. LIE AND S.NOELLE, *On the artificial compression method for second-order nonoscillatory central difference schemes for systems of conservation laws*, SIAM J. Sci. Comput., 24 (2003), pp. 1157–1174.
[13] X.-D. LIU, S. OSHER AND T. CHAN, *Weighted essentially non-oscillatory schemes*, J. Comput. Phys., 115 (1994), pp. 200–212.
[14] X.-D. LIU AND E. TADMOR, *Third order nonoscillatory central scheme for hyperbolic conservation laws*, Numer. Math., 79 (1998), pp. 397–425.
[15] H. NESSYAHU AND E. TADMOR, *Non-oscillatory central differencing for hyperbolic conservation laws*, J. Comput. Phys., 87 (1990), pp. 408–463.
[16] P.K. SWEBY, *High resolution schemes using flux limiters for hyperbolic conservation laws*, SIAM J. Numer. Anal., 21 (1984), pp. 995–1011.
[17] E.F. TORO, *Riemann solvers and numerical methods for fluid dynamics*, Springer, Berlin, Heidelberg, 1997.

DEPARTMENT OF PHYSICS AND MATHEMATICS DEPARTMENT, TULANE UNIVERSITY
6823 ST. CHARLES AVE., NEW ORLEANS, LA 70118, USA
E-mail address: lconstan@tulane.edu

MATHEMATICS DEPARTMENT, TULANE UNIVERSITY
6823 ST. CHARLES AVE., NEW ORLEANS, LA 70118, USA
E-mail address: kurganov@math.tulane.edu